Exposure to per- and polyfluoroalkyl substances elicits cell type-specific impacts on p53 and TGF-β signaling pathways

Hongran Ding[1,3], Maya Slack[2,3], Holly McClure[2,3], Wen Gu[2,3], Carly Nabinger[2,3], Renata Koviazina[2,3], Helene Gu[2,3], Ferdinand Kappes[2], Thomas F. Schultz[4], Jason A. Somarelli[5], Anastasia Tsigkou[2,3]

[1] Duke Kunshan University, Masters of Global Health Program, Kunshan,China
[2] Duke Kunshan University, Division of Natural and Applied Sciences, Kunshan, China
[3] Duke Kunshan University, Reproductive Oncology Lab, Kunshan, China
[4] Duke University, Nicholas School of the Environment, Durham, NC, USA
[5] Duke University, Department of Medicine, Durham, NC, USA

Corresponding Author:
Anastasia Tsigkou, anastasia.tsigkou@duke.edu (ORCID ID 0000-0001-5195-5673);
Co-Corresponding Author:
Jason Somarelli, jason.somarelli@duke.edu (ORCID ID 0000-0003-1510-9343)

Keywords: Plastic Pollution, PFOA, GenX, Cytotoxicity, TGFB, SMAD

Graphical Abstract

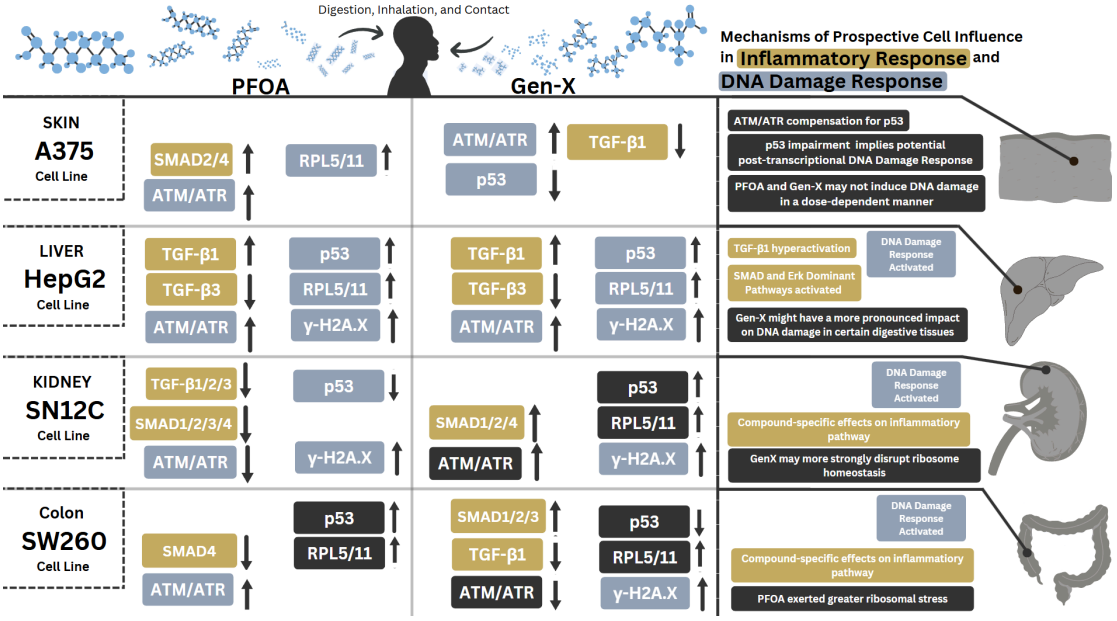

Abstract

Per- and polyfluoroalkyl substances (PFAS) are a class of synthetic chemicals extensively used as plastic additives. Their environmental persistence and potential for bioaccumulation have raised significant toxicological concerns. This study evaluates the cytotoxic and molecular effects of Perfluorooctanoic acid (PFOA) and its replacement compound, Perfluoro(2-methyl-3-oxohexanoic) acid (Gen-X), in human-derived skin (A375), liver (HepG2), kidney (SN12C), and colon (SW620) cell lines. We assessed cell viability, gene expression, and perturbations in key cellular stress pathways, with a particular focus on TGF-β/SMAD-mediated inflammation and the p53-driven DNA damage response.

Our results demonstrate compound- and cell-type-specific toxicity, with Gen-X displaying reduced cytotoxicity compared to PFOA across all cell types. Molecular analyses revealed that both PFAS compounds induced alterations in the TGF-β/SMAD pathway, consistent with a pro-inflammatory cellular state. Additionally, we observed activation of the DNA damage response, as evidenced by increased expression of γ-H2A.X, ATM, ATR, and p53, alongside ribosomal stress-related changes in RPL5 and RPL11. Notably, while skin and liver cells exhibited similar response profiles, kidney and colon cells showed divergent modulation of SMAD signaling, suggesting tissue-specific susceptibility and mechanistic differences.

These findings contribute to a deeper understanding of the differential toxicological profiles of legacy and replacement PFAS, with implications for health risk assessment and regulatory policy.

Introduction

Per- and polyfluoroalkyl substances (PFAS) are a series of synthetic organic fluorides that are intended as water resistant and non-stick coatings and used as additives to plastic and other materials (Buck et al. 2011). These properties are desirable for consumer applications such as cosmetics, food packaging, pesticides, water repellent textiles, and medical devices (De Silva et al., 2021; Omotola et al., 2024). However, in the process of manufacturing and waste disposal, PFAs can be released to the atmosphere and water sources (Ehsan et al., 2023). Due to their remarkably stable chemical structures, PFAS decay at a slow rate, leading to persistence of PFAS in water, soil, and air (Kwiatkowski et al., 2020) and bioaccumulation of PFAS substances in living organisms (Buck et al., 2011).

PFAS monitoring suggests widespread exposure among various global human populations (Liu et al., 2020; Poothong et al., 2020). For example, analysis of human biospecimens from Guangdong Province in China detected eleven PFAS substances, with mean concentrations of 3.6 $ng*mL^{-1}$ and 5.4 $ng*g^{-1}$, of PFOA in hair and nails, respectively (Liu et al., 2020). Similarly, a study in Norway detected daily intake of 18 PFAS compounds and 12 PFAS precursors, where PFOS and PFOA were the predominant PFAS in serum (Poothong et al., 2020).

Among the more than 10,000 PFAS chemicals, perfluorooctanoic acid (PFOA) is one of the most common and well-known chemicals in this class. In the environment, PFOA levels can reach 1.490 ng/g - 8.0 ng/g in soil (Omotola et al., 2024; Xiao et al., 2015) and can leach into groundwater, with levels from 0.1 ng/L in remote areas to 3.9 ng/L in urban areas, and some areas, such as the Yangtze River in China with median PFOA levels of up to 297.5 ng/L at some sites (Jin et al., 2009).

Previous studies of PFOA exposure have found multiple impacts on cell and organismal health, including immunotoxicity(Sunderland et al., 2019) endocrine disruption and metabolic abnormalities and dyslipidemia (Ubel et al., 1980). Consistent with this, human studies show an association between PFOA and metabolic abnormalities, such as high cholesterol and hyperuricemia (Lin et al. 2013). Previous animal studies also show PFOA accumulates in the liver, causing hepatocellular hypertrophy (Gomis et al., 2018). In the context of these health impacts, the 2019 International Stockholm Convention on Persistent Organic Pollutants resulted in a nearly global ban of PFOA (Wee and Aris, 2023).

Gen-X is a new generation of PFAS. With a shorter environmental retention time due to its shorter chain and ether group, it was regarded as a safer alternative to PFOA in the early 2000s (Zane and Schultz, 2020). However, recent animal model studies have suggested Gen-X to be hepatotoxic (Gomis et al., 2018). It may also upregulate the peroxisome proliferator-activated receptor (PPAR) pathway, affecting lipolysis, fatty acid uptake, and lipoprotein mechanisms (Conley et al., 2019). Additionally, exposure induces apoptosis in liver cells and may have epigenetic toxicity (Yoo et al., 2021). In many studies, Gen-X has been termed as a “regrettable substitute” requiring further research to discern its potentially more harmful impacts (Ahearn, 2019).

To better understand the effects of exposure to PFOA (perfluorooctanoic acid) and Gen-X in relation to DNA damage, cytotoxicity, and the potential for carcinogenic outcomes, we evaluated the two chemicals across multiple cell lines. We focused on comparing γH2AX expression, a well-established marker for DNA double-strand breaks (DSBs), along with key molecular pathways involved in stress responses, including ribosomal stress and TGF-β/SMAD signaling as outlined in

Figure 1.

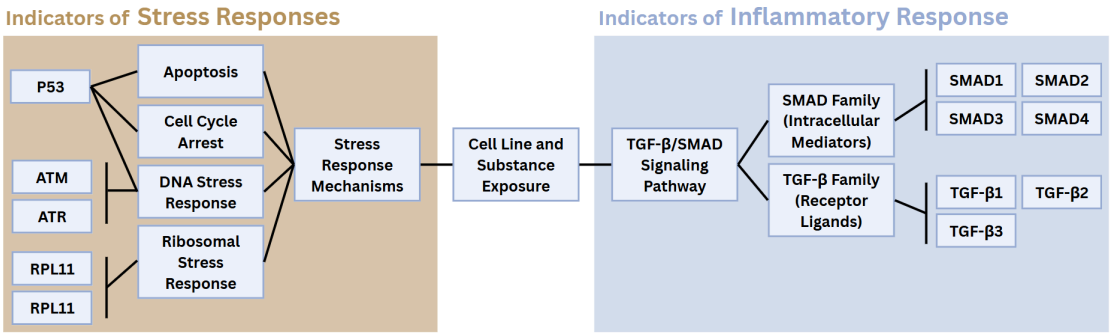

Figure 1. Key Genes and Pathways Linking DNA Damage Response, Ribosomal Stress, and TGF-β/SMAD Signaling in Tumor Microenvironment Regulation

This figure highlights key genes and proteins examined in the study. The DNA damage response is represented by **p53**, **ATM**, and **ATR** genes, along with **γ-H2A.X** protein, a marker of DNA double-strand breaks. **RPL5** and **RPL11**, both ribosomal proteins, are involved in p53 regulation through the nucleolar stress response. The **TGF-β/SMAD signaling pathway**, a critical regulator of immune response and inflammation, is also depicted due to its role in modulating the tumor microenvironment.

Methods

Detailed information about chemicals and materials used can be found in Appendices 1-3.

Cell culture and analysis of cytotoxicity

Four adherent cell lines—A375 (melanoma), HepG2 (hepatocellular carcinoma), SN12C (renal cell carcinoma), and SW620 (colorectal cancer)—were used in this study. All cells were initially cultured in T25 flasks and subsequently transferred to T75 flasks at the third passage. The culture medium consisted of Dulbecco's Modified Eagle Medium (DMEM) supplemented with 10% fetal bovine

serum (FBS) and 1% penicillin-streptomycin (P/S). Flasks were maintained in a humidified incubator at 37 °C, 5% CO_2, pH 7.4, and 95% relative humidity. All media tested negative for mycoplasma contamination prior to experimentation.

Cytotoxicity was assessed by Cell Counting Kit-8 (CCK-8). Cells (4,000 per well) were seeded in 96-well plates for 24 hours and culture medium was replaced with fresh medium containing defined concentrations of PFOA (0, 100, 250, 500, 750, and 1,000 μM) or Gen-X (0, 500, 1,000, 2,000, 3,000, and 4,000 μM). Both PFOA and Gen-X were dissolved in DMSO at the final concentrations of 0.1M and 1M respectively, and stored at -20°C (Abudayyak et al., 2021). The control group was treated with complete medium containing 1% DMSO. After 48 hours of toxicity exposure, cell viability assay using CCK-8 was performed. 10 μL of enhanced CCK-8 solution was added to each well, including the control wells for determination of background. Incubation was continued for 2 hours in a cell culture incubator, followed by measurement of absorbance at 450 nm using a Varioskan™ LUX plate reader. IC_{50} values were attained by nonlinear regression of at least three biological replicates. Goodness of fit values (R^2) were also calculated for each regression.

Protein extraction

0.1 mL of cells diluted to $5*10^4$ cells/mL were seeded into 6-well plates and exposed to concentrations of PFOA and Gen-X for 48 hours at concentrations representing 1/2 IC_{50}, IC_{50}, or $2*IC_{50}$, whereas 1% DMSO served as control. Cells were then washed with ice-cold PBS and cell lysis was achieved by addition of 200 μL RIPA lysis buffer per well, containing 1 mM Phenylmethylsulfonyl fluoride (PMSF). Six six-well plates were placed on ice for 10 minutes to allow for complete cell lysis followed by transfer of lysates to 1.5 mL centrifuge tubes and centrifugation at 12,000x-g for 5 min. Supernatants containing extracted proteins were then stored at

-80°C.

Immunoblotting

Immunoblotting was carried out as described previously (Hu et al., 2020). To standardize protein concentrations among lysates, the Enhanced BCA Protein Assay Kit was used and a total of 20 - 30 uL of total protein were loaded in SDS-PAGE gels (Appendix 2), and electrophoresis of samples was performed in a gel electrophoresis system with running buffer (Appendix 2) along a protein size marker (10-180 kDa). Separated proteins were transferred to a PVDF membrane using a wet transfer system and transfer buffer (Appendix 1). Resulting membranes were blocked on an orbital shaker for 1h at room temperature by adding a blocking buffer (5% BSA dissolved in TBST, Appendix 2). and incubated with primary and secondary antibodies diluted in TBST containing 1% BSA, with ratios in Appendix 3. The membranes were imaged using a chemiluminescence imaging system.

RNA extraction and cDNA synthesis

Total RNA extraction using Trizol reagent has been described in detail in previous research and follows standard protocols (Gandhi et al., 2020). For cDNA synthesis, the HiScript II 1st Strand cDNA Synthesis Kit was used. RNA concentration was estimated using Nanodrop. First-strand cDNA synthesis reaction solutions were assembled in RNase-free centrifuge tubes with a total of 1 μg RNA per sample. The reaction solutions were mixed gently and sequentially reacted at 25°C for 5 min, 50°C for 15 min, and 85°C for 2 min in a PCR thermal cycler.

Quantitative PCR

All quantitative (q)PCR experiments were performed using 96-well PCR plates. In the 20 μL reaction system, 10 μL was ChamQ Universal SYBR qPCR Master Mix, 0.4 μL of 1 μM forward primer, 0.4 μL of 1 μM reverse primer, 7.2 μL of

RNase-free ddH_2O, and 2 μL of template cDNA. Primer details are shown in Appendix 4. The qPCR thermal cycler was set as 95℃ for 30 seconds with 1 repetition (Pre-denaturation), 95℃ 10 seconds and 60℃ 30 seconds with 40 repetitions (Cycling Reactions), and a melting curve acquisition (Default melting curve program). Relative expression was calculated using the 2^-ΔΔCt method.

Statistical analysis

All cytotoxicity results are presented as a value and 95% confidence interval while qPCR results are presented as mean ± standard deviation (SD). Data were analyzed by two-tailed t-tests for groups with 2 variables and analysis of variance (ANOVA) for groups with more than 2 variables. GraphPad Prism version 9.5.1 for Windows was used. P-values < 0.05 were considered significant.

Results

Cytotoxicity assessment

All cells were more tolerant to Gen-X and displayed similar trends in cytotoxicity. IC_{50}'s ranged from 213.2 μM to 5048 μM, with highest sensitivity observed in A375 and SW620 cells and lower sensitivity in HepG2 and SN12C cells . The A375 cell line showed a high sensitivity to PFOA with an IC_{50} value of 213.2 μM ($R^2 = 0.9375$) (Fig. 1A) and more tolerance to Gen-X with an IC_{50} value of up to 1555 μM ($R^2 = 0.9920$) (Fig. 1B). HepG2 cells were moderately low in sensitivity to PFOA with an IC_{50} of 527.9 μM ($R^2 = 0.9974$) (Fig. 1A). Overall, all cell types were more resistant to Gen-X exposure with an average estimated IC_{50} value of 2377 μM ($R^2 = 0.9747$) (Fig. 1B). SN12C cells showed the most resistance overall, with an IC_{50} value of 616.3 μM for PFOA and IC_{50} values up to 5,048 μM ($R^2 = 0.9400$) for Gen-X (Fig. 1B). The SW620 cell line exhibited moderate sensitivity to PFOA with an IC_{50} of 271.2 μM ($R^2 = 0.9965$) (Fig. 1A). Similarly, SW620 also showed moderate tolerance

to Gen-X with an IC_{50} of 2126 μM ($R^2 = 0.9874$) (Fig. 1B).

A) Cytotoxicity of PFOA

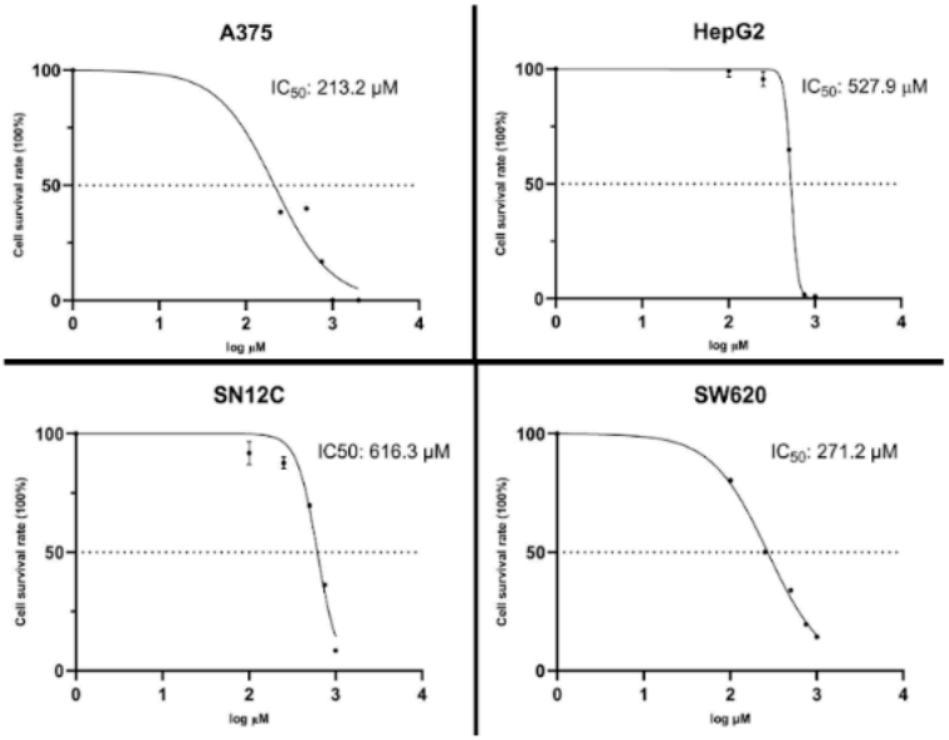

B) Cytotoxicity of Gen-X

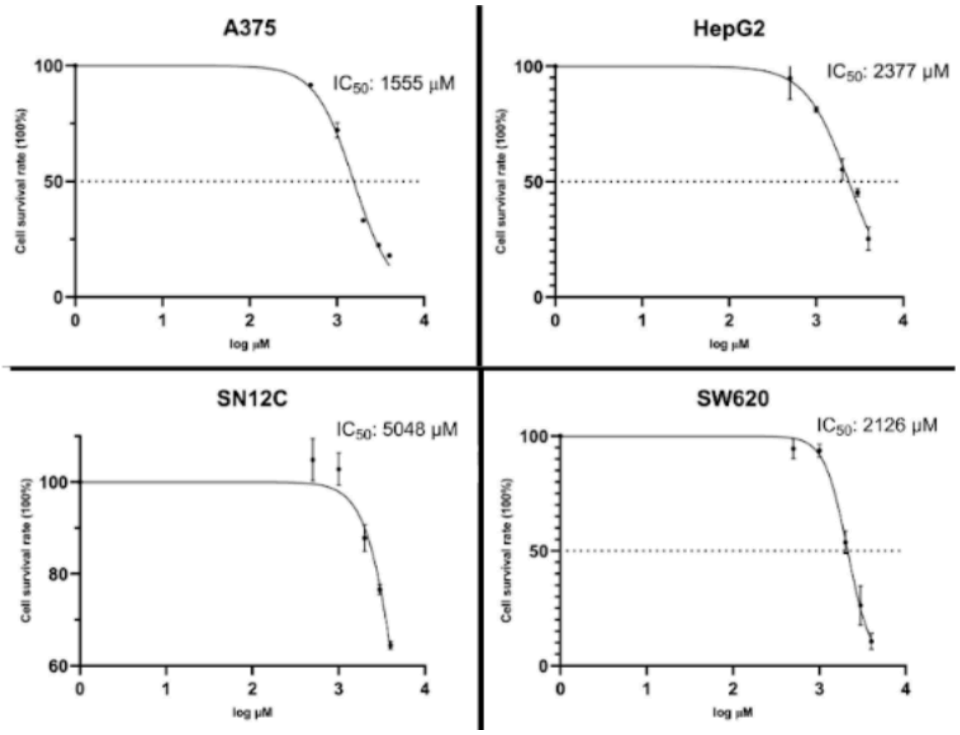

Figure 2: Viability of A375, SN12C, SW620, and HepG2 cells including A) Cytotoxicity to PFOA and B) Cytotoxicity to Gen-X.

The data obtained through CCK-8 experiments were transformed to a log base after processing, fitted

using nonlinear regression, and resulted in cell viability curves for each cell in response to PFOA concentration. Dashed lines represent the PFOA concentration at which half of the cells survived (IC_{50}), and the best-fit values are labeled in the upper right corner.

Table 1: IC_{50} of A375, HepG2, SN12C, and SW620 cell stress response to PFOA and Gen-X

IC50 values were obtained by CCK-8 assay, and estimated by fitting the results using nonlinear regression with a 95% confidence interval range.

Cell lines	PFOA treated IC_{50} µM (95% CI)	Gen-X treated IC_{50} µM (95% CI)
A375	213.2 [23.54, 393.8]	1555 [1452, 1664]
HepG2	527.9 [514.6*, 541.2]	2377 [2148, 2630]
SN12C	616.3 [558.8, 670.1]	5048 [4451, 6193**]
SW620	271.2 [239.8, 304.4]	2126 [1984, 2267]

* Unable to estimate specific values
** Unable to estimate specific values due to exceeding limit set

Cell Line Exposure effects on Inflammatory and Stress Responses Focusing on TGF-β/SMAD Pathway

Having established acute cytotoxicity estimates for PFOA and Gen-X, we sought to understand the molecular consequences of exposure, with focus on DNA damage/repair (γ-H2A.X, ATM/ATR, P53 expression), ribosomal stress (RPL5/11) and immune signaling (TGF-β/SMAD pathway). We found effects to differ between the two chemicals as well as between cell lines (Figs. 3, 4, 5, 6). Changes in gene expression and protein level are summarized in Table 2.

i) A375 cell line

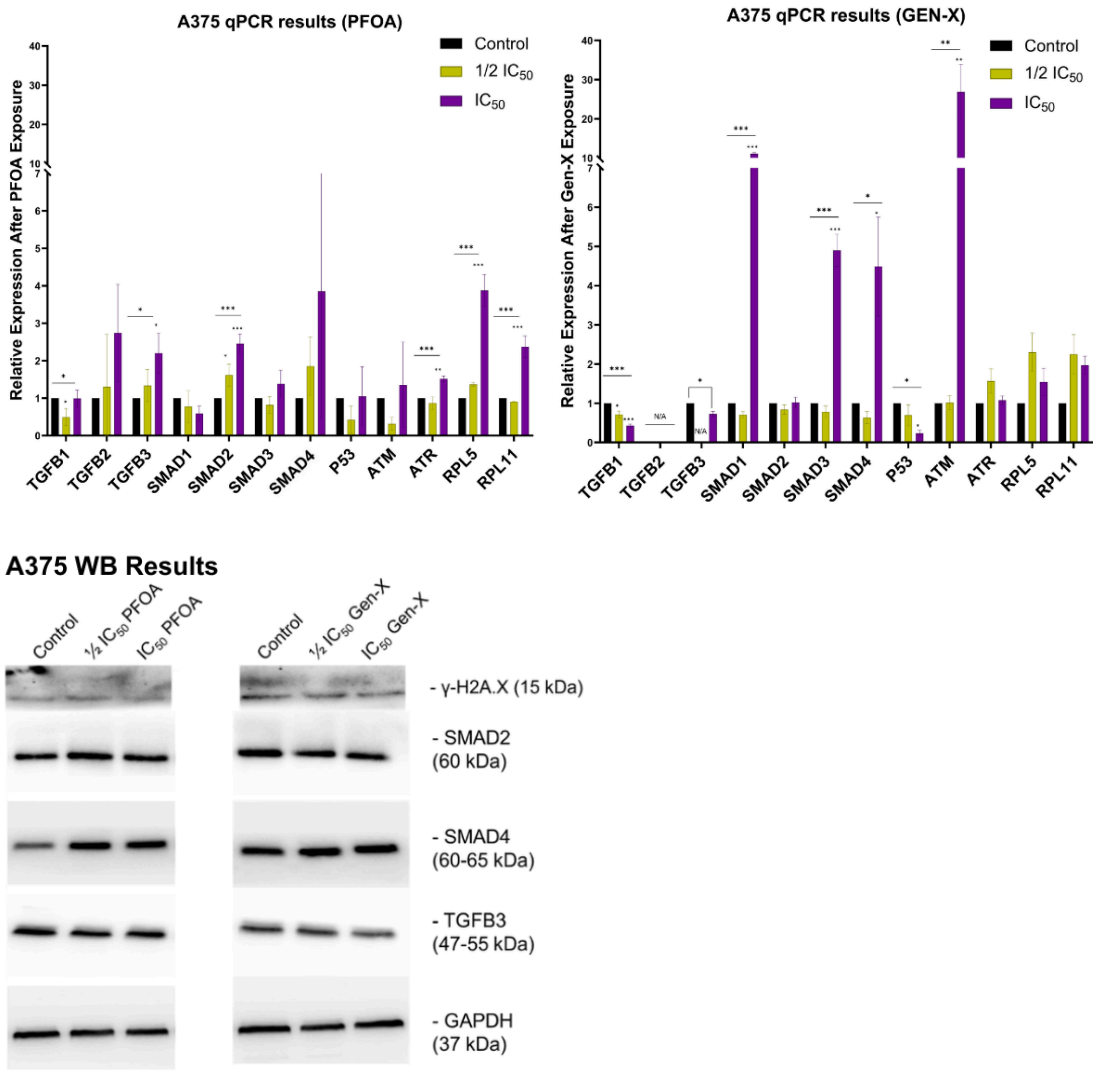

Figure 3. Altered gene and protein expression in A375 cells following PFOA or Gen-X treatments

A375 cells were treated with vehicle, A) PFOA or B) Gen-X with concentration of 1/2 IC_{50}, IC_{50} for 48 h and relative mRNA levels were determined by RT-qPCR. *, $p < 0.05$; **, $p < 0.01$, *** $p < 0.001$ C) The WB results of target inflammatory response proteins extracted from the control group and PFOA or Gen-X treated A375 cells with concentration of 1/2 IC_{50}, IC_{50}.

Exposure of A375 cells to PFOA increased SMAD2 gene expression with $p < 0.05$ (Fig. 3A) and SMAD4 protein level in both ½ IC_{50} and IC_{50} concentrations,

while no significant trend was observed for the expression of other proteins (Fig. 3C). As shown in Figure 3A, more significant changes in the expression of genes occurred at the IC_{50} . At ½ IC_{50} , $TGF\beta_1$ gene expression decreased ($p < 0.05$), while SMAD2 gene expression increased. At IC_{50} , $TGF\beta_1$ gene increased on the contrary ($p < 0.05$), along with increases in $TGF\beta_3$ ($p < 0.05$), SMAD2, ATR, RPL5, and RPL11 ($p < 0.001$) compared to untreated controls. However, the expression of other genes such as p53, ATM, $TGF\beta_2$, $TGF\beta_3$, SMAD1 and SMAD3 did not change significantly in the experimental group. Furthermore, there was no observed change in γ-H2A.X after either PFOA or Gen-X treatment (Fig. 3C).

In the Gen-X treated A375 cells, the expression of $TGF\beta_1$ was decreased at ½ IC_{50} concentration compared to the control (Fig. 3B). At ½ IC_{50} there were no other significant gene expression or protein level changes. At $IC_{50,}$ there were more changes again. In the TGF-β family genes, $TGF\beta_1$ gene expression decreased at IC_{50}-treated concentrations ($p < 0.001$), and the expression of $TGF\beta_3$ increased significantly at both ½ IC_{50} and IC_{50} concentrations ($p < 0.05$ and $p < 0.001$), while $TGF\beta_2$ did not show a corresponding signal in the experiment (N/A). In the SMAD family genes, SMAD1, SMAD3 and SMAD4 showed significant up-regulation ($p < 0.001$ for SMAD1, SMAD3 and $p < 0.05$ for SMAD4), which is consistent with the activation of the TGF-β signaling pathway. The expression of SMAD2 did not show statistically significant changes after Gen-X treatment. In addition, ATM also showed a significant increase in expression at IC_{50} concentrations ($p < 0.01$), suggesting that a DNA damage response mechanism may have been induced in the presence of Gen-X. However, the p53 gene showed a decrease in expression at IC_{50} concentration ($p < 0.05$).

ii) HepG2 cell line

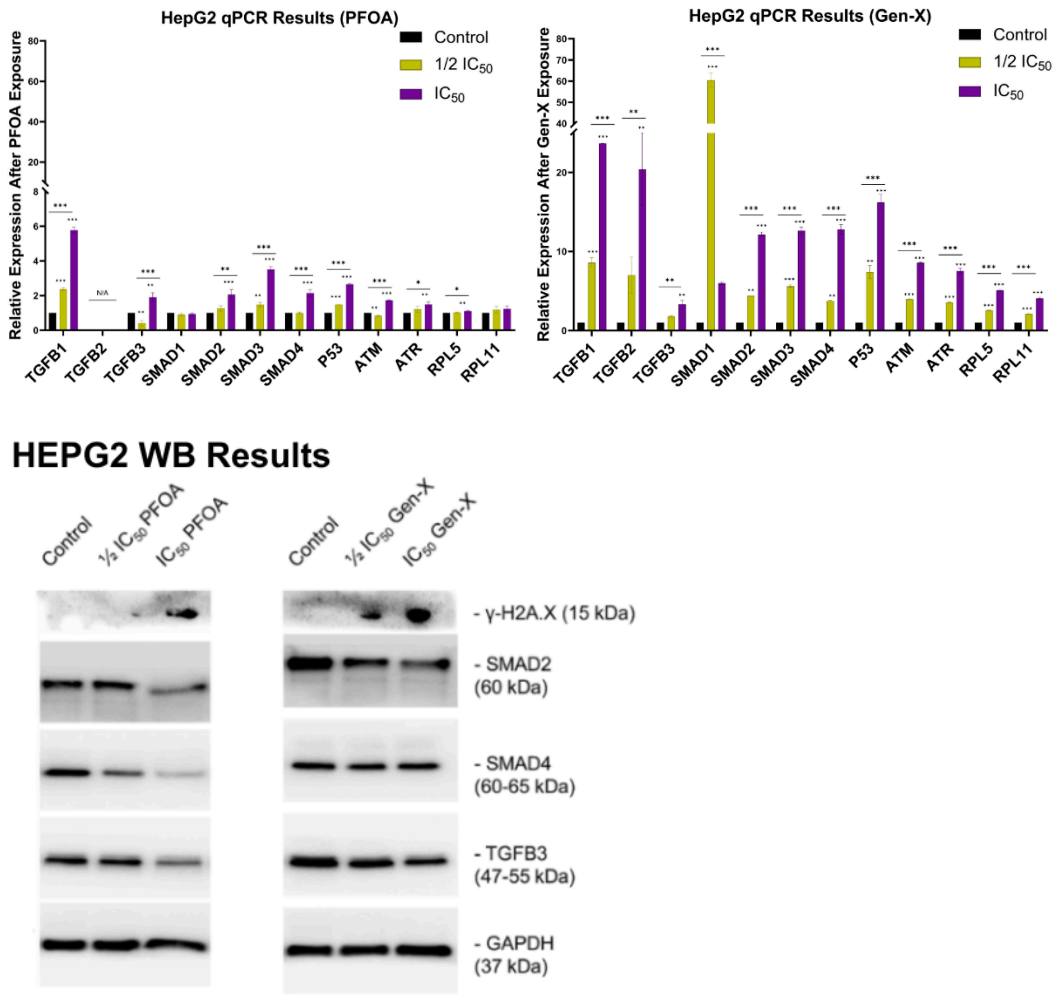

Figure 4. Altered gene and protein expression in HepG2 cells following PFOA or Gen-X treatments

HepG2 cells were either mock-treated or treated with A) PFOA or B) Gen-X with concentration of 1/2 IC_{50}, IC_{50} for 48 h and relative mRNA levels were determined by q-PCR. *, $p < 0.05$; **, $p < 0.01$, *** $p < 0.001$; C) The WB results of target inflammatory response proteins extracted from the control group and PFOA or Gen-X treated HepG2 cells with concentration of 1/2 IC_{50}, IC_{50}.

In the HepG2 liver cell line, there were significant changes caused by both chemicals at 1/2 IC_{50} and IC_{50} levels. These effects were generally similar between PFOA and Gen-X.

For exposure to PFOA at 1/2 IC_{50} the expression of the $TGF\beta_1$ gene was more

than 2-fold higher ($p<0.001$). SMAD3 ($p<0.01$), p53 ($p<0.001$), and ATM ($p<0.01$) gene expression also increased. Both TGFβ_3 gene ($p<0.05$) and proteins expressed less at ½ IC_{50} as well as SMAD2 and SMAD4 protein levels (Fig. 4C). No γ-H2A.X band was observed in the control group, but its expression increased with increasing toxin concentrations. At IC_{50} the TGFβ_1 gene expression increased again to around 6-fold higher than the control ($p<0.001$). SMAD2 ($p<0.01$), SMAD3 ($p<0.001$), SMAD4 ($p<0.001$), ATM ($p<0.001$), ATR ($p<0.05$), and RPL5 ($p<0.05$) gene expressions also increased. Interestingly, TGFβ_3 , downregulated at ½ IC50, increased to 2-fold compared to the control group at IC50 ($p < 0.001$). However, the TGFβ_3 protein levels decreased, along with SMAD2 and SMAD4 proteins, despite their respective gene upregulations. The expression data for TGFβ_2 were not applicable to this analysis as the signal from the control could not be observed (N/A).

In the Gen-X treatment group (Fig. 4B), all target gene expressions showed increases in different degrees. Specifically, both TGFβ_1 and TGFβ_2 expressed more than 20-fold higher at IC_{50} ($p<0.001$ and $p<0.01$ respectively). The SMAD1 expression showed the greatest increase at the ½ IC_{50} concentration ($p<0.001$), but its increase at the IC_{50} concentration is not statistically significant. At ½ IC_{50} TGFβ_1 ($p<0.001$), SMAD1 ($p<0.001$), SMAD2 ($p<0.01$), SMAD4 ($p<0.01$), p53 ($p<0.01$). ATM ($p<0.001$), ATR ($p<0.001$), RPL5 ($p<0.001$), RPL11 ($p<0.001$) gene expression and γ-H2A.X protein increased, while the TGFβ3 and SMAD2 proteins decreased. At IC_{50} TGFβ_1 ($p<0.001$), TGFβ_2 ($p<0.01$), TGFβ_3 ($p<0.01$), SMAD2, SMAD3, SMAD4, p53, ATM, ATR, RPL5, and RPL11 (all $p<0.001$) gene expression, and γ-H2A.X protein increased. The γ-H2A.X showed an increasing trend with increasing Gen-X concentration. TGFβ3 and SMAD2 proteins showed a decreasing trend with increasing Gen-X concentration.

iii) SN12C cell line

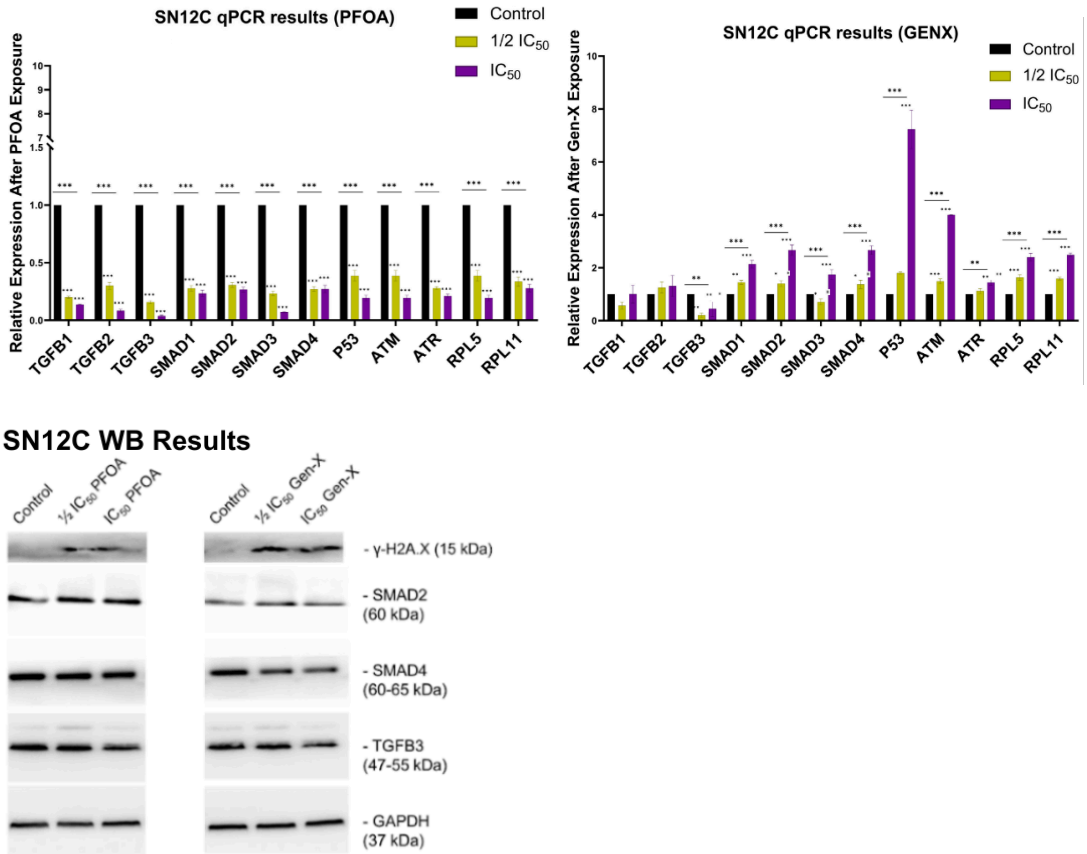

Figure 5. Altered gene and protein expression in SN12C cells following PFOA or Gen-X treatments
SN12C cells were either mock-treated or treated with A) PFOA or B) Gen-X with concentration of 1/2 IC_{50}, IC_{50} for 48 h and relative mRNA levels were determined by q-PCR. *, $p < 0.05$; **, $p < 0.01$, *** $p < 0.001$; C) The WB results of target inflammatory response proteins extracted from the control group and PFOA or Gen-X treated SN12C cells with concentration of 1/2 IC_{50}, IC_{50}.

In the SN12C cell line, the expression of genes associated with TGFβ pathway, cellular stress response, DNA damage repair,ribosome assembly, and immune signaling all significantly decreased after PFOA treatment with both the ½ IC_{50} and IC_{50} concentrations of PFOA, and the expression of these genes was particularly more pronounced at IC_{50} concentrations, with the statistical significance reaching the level of $p < 0.001$ (Fig. 5A). Notably, despite decreases in gene

expression, SMAD2 and SMAD4 protein concentrations didn't change. Also, γ-H2A.X cannot be observed in the control group and the abundance increased gradually with the increase of toxin exposure in both treatment groups.

In contrast, under Gen-X treatment (Fig. 5B), all genes other than $TGF\beta_1$, $TGF\beta_2$,and $TGF\beta_3$ all showed a significant increase in expression at IC_{50} concentration ($p < 0.001$). SMADs, ATM/ATR, RPL5/RPL11, and especially p53 showed a dose-dependent increase trend with increasing Gen-X. However, with the TGFβ family, $TGF\beta_3$ was decreased in expression at ½ IC_{50} and IC_{50} concentrations from the control, while $TGF\beta_1$ and $TGF\beta_2$ were unchanged. There was also an upward trend in SMAD2 protein levels and a decreased trend in SMAD4 protein levels in response to escalating Gen-X concentrations.

iv) SW620 cell line

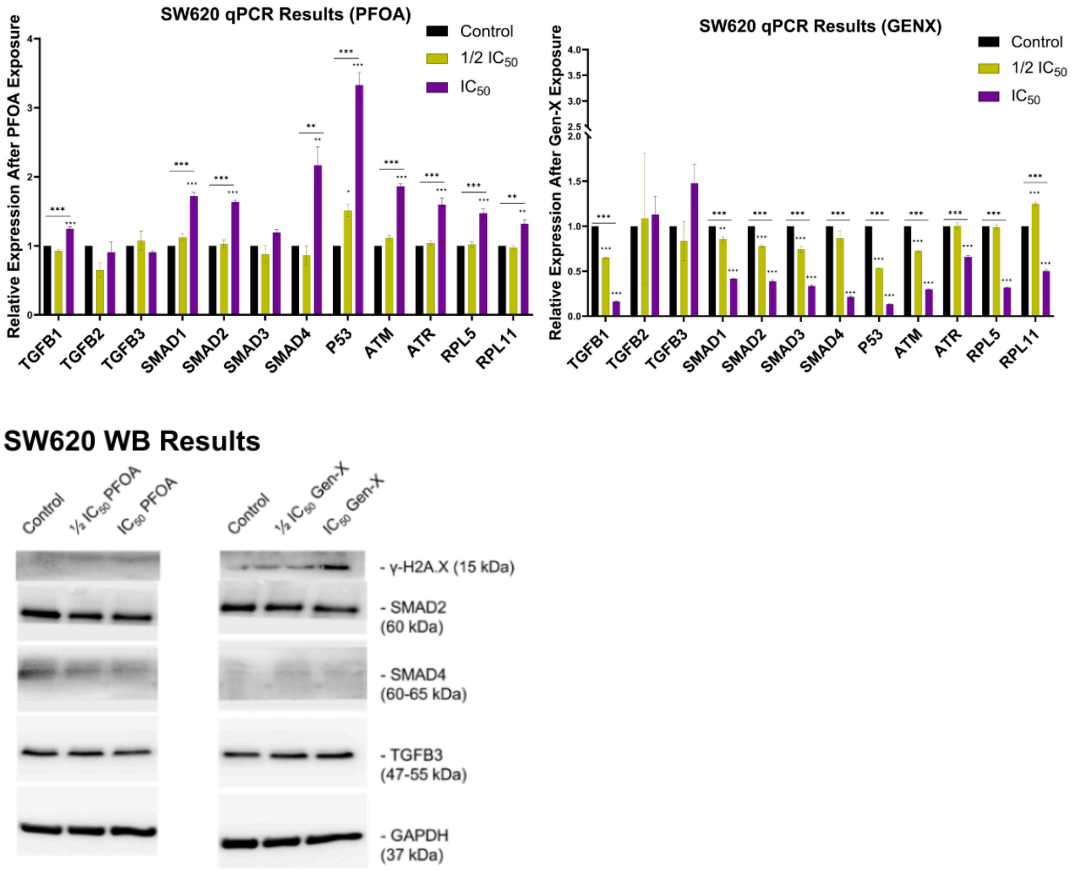

Figure 6. Altered gene and protein expression in SW620 cells following PFOA or Gen-X

treatments

SW620 cells were either mock-treated or treated with A) PFOA or B) Gen-X with concentration of 1/2 IC_{50}, IC_{50} for 48 h and relative mRNA levels were determined by q-PCR. *, $p < 0.05$; **, $p < 0.01$, *** $p < 0.001$; C) The WB results of target inflammatory response proteins extracted from the control group and PFOA or Gen-X treated SW620 cells with concentration of 1/2 IC_{50}, IC_{50}.

In the SW620 cell line, p53 mRNA was significantly upregulated, and SMAD4 protein levels decreased. At IC_{50} SMAD4 protein levels continued to decrease, but the $TGF\beta_1$ ($p < 0.001$), SMAD1 ($p < 0.001$), SMAD2 ($p < 0.001$), and SMAD4 ($p < 0.01$) genes exhibited increased expression at the IC_{50} concentration. Levels of p53, ATM, ATR, RPL5, and RPL11 mRNAs were increased by treatment with PFOA at the IC_{50} concentration.

In the Gen-X treatment group (Fig. 6B), the target gene expressions showed an overall decreasing trend. Within the TGF-β family, there was a significant decrease in $TGF\beta_1$ in both groups ($p<0.001$). The expression of $TGF\beta_2$ and $TGF\beta_3$ increased but did not show statistical significance. The expression of SMAD family genes was also significantly affected by Gen-X treatment. At ½ IC_{50} a decrease in $TGF\beta_1$, SMAD1, SMAD2, SMAD3, p53, and ATM, while RPL11 increased ($p<0.001$ for all except $p<0.01$ for SMAD1). At IC_{50} , maybe gene expressions continued to decrease, such as $TGF\beta_1$, SMAD1, SMAD2, SMAD3, SMAD4, p53, ATM, ATR, and RPL5 ($p<0.001$ from control for all). After increasing with exposure to ½ IC_{50} , RPL11 decreased to be below the levels of the control with IC_{50} exposure ($p<0.001$). Although there was no observable change in γ-H2A.X levels with PFOA, the abundance of γ-H2A.X increased with the increase of the concentration in the Gen-X exposed group. Interestingly, no Gen-X induced protein level changes were observed besides this γ-H2A.X trend (Fig. 6C).

Table 2: Summary of Gene and Protein Expression of Inflammatory and DNA Stress Response Markers

This table summarizes the changes in gene expression (measured by qPCR) and protein levels (measured by immunoblot/western blot) of target inflammatory and stress response markers. Unless otherwise specified with "protein", entries in the table refer to the gene expression. *, $p < 0.05$; **, $p < 0.01$, *** $p < 0.001$. Yellow indicates a decrease while blue indicates an increase in expression.

	½ IC50		IC50	
Skin A375	PFOA	Gen-X	PFOA	Gen-X
	TGFβ1 ↓* TGFβ2 — TGFβ3 — TGFβ3 protein — SMAD 1 — **SMAD 2 ↑*** SMAD 2 protein — SMAD 3 — SMAD 4 — **SMAD 4 protein ↑** P53 — ATM — ATR — RPL5 — RPL11 — γ-H2A.X protein —	**TGFβ1 ↓*** TGFβ2 — TGFβ3 — TGFβ3 protein — SMAD 1 — SMAD 2 — SMAD 2 protein — SMAD 3 — SMAD 4 — SMAD 4 protein — P53 — ATM — ATR — RPL5 — RPL11 — γ-H2A.X protein —	**TGFβ1 ↑*** TGFβ2 — **TGFβ3 ↑*** TGFβ3 protein — SMAD 1 — **SMAD 2 ↑***** SMAD 2 protein — SMAD 3 — SMAD 4 — **SMAD 4 protein ↑** P53 — ATM — **ATR ↑***** **RPL5 ↑***** **RPL11 ↑***** γ-H2A.X protein —	**TGFβ1 ↓***** TGFβ2 — **TGFβ3 ↓*** TGFβ3 protein — **SMAD 1 ↑***** SMAD 2 — SMAD 2 protein — **SMAD 3 ↑***** **SMAD 4 ↑*** SMAD 4 protein — **P53 ↓*** **ATM ↑****** ATR — RPL5 — RPL11 — γ-H2A.X protein —

	½ IC50		IC50	
Liver HepG2	**TGFβ1 ↑***** TGFβ2 — **TGFβ3 ↓*** **TGFβ3 protein ↓** SMAD 1 — SMAD 2 — **SMAD 2 protein ↓** **SMAD 3 ↑**** SMAD 4 — **SMAD 4 protein ↓** **P53 ↑***** **ATM ↑**** ATR — RPL5 — RPL11 — **γ-H2A.X protein ↑**	**TGFβ1 ↑***** TGFβ2 — TGFβ3 — **TGFβ3 protein ↓** **SMAD 1 ↑***** **SMAD 2 ↑**** **SMAD 2 protein ↓** SMAD 3 — **SMAD 4 ↑**** SMAD 4 protein — **P53 ↑**** **ATM ↑***** **ATR ↑***** **RPL5 ↑***** **RPL11 ↑***** **γ-H2A.X protein ↑**	**TGFβ1 ↑***** TGFβ2 — **TGFβ3 ↑***** **TGFβ3 protein ↓** SMAD 1 — SMAD 2 ↑** **SMAD 2 protein ↓** **SMAD 3 ↑***** **SMAD 4 ↑***** **SMAD 4 protein ↓** P53 — **ATM ↑***** **ATR ↑*** **RPL5 ↑*** RPL11 — **γ-H2A.X protein ↑**	**TGFβ1 ↑***** **TGFβ2 ↑**** **TGFβ3 ↑**** **TGFβ3 protein ↓** SMAD 1 — **SMAD 2 ↑***** **SMAD 2 protein ↓** **SMAD 3 ↑***** **SMAD 4 ↑***** SMAD 4 protein — **P53 ↑***** **ATM ↑***** **ATR ↑***** **RPL5 ↑***** **RPL11 ↑***** **γ-H2A.X protein ↑**
Kidney SN12C	PFOA	Gen-X	PFOA	Gen-X
	TGFβ1 ↓*** **TGFβ2 ↓***** **TGFβ3 ↓***** **TGFβ3 protein ↓** **SMAD 1 ↓***** **SMAD 2 ↓***** SMAD 2 protein — **SMAD 3 ↓***** **SMAD 4 ↓***** SMAD 4 protein — **P53 ↓***** **ATM ↓***** **ATR ↓***** **RPL5 ↓***** **RPL11 ↓***** **γ-H2A.X protein ↑**	TGFβ1 — TGFβ2 — **TGFβ3 ↓**** **TGFβ3 protein ↓** **SMAD 1 ↑**** **SMAD 2 ↑*** **SMAD 2 protein↑** **SMAD 3 ↓*** **SMAD 4 ↑*** **SMAD 4 protein↓** P53 — **ATM ↑***** ATR — **RPL5 ↑***** **RPL11 ↑***** **γ-H2A.X protein ↑**	**TGFβ1 ↓***** **TGFβ2 ↓***** **TGFβ3 ↓***** **TGFβ3 protein ↓** **SMAD 1 ↓***** **SMAD 2 ↓***** SMAD 2 protein — **SMAD 3 ↓***** **SMAD 4 ↓***** SMAD 4 protein — **P53 ↓***** **ATM ↓***** **ATR ↓***** **RPL5 ↓***** **RPL11 ↓***** **γ-H2A.X protein ↑**	TGFβ1 — TGFβ2 — **TGFβ3 ↑*** **TGFβ3 protein ↓** **SMAD 1 ↑***** **SMAD 2 ↑***** **SMAD 2 protein↑** **SMAD 3 ↑***** **SMAD 4 ↑***** **SMAD 4 protein↓** **P53 ↑***** **ATM ↑***** **ATR ↑**** **RPL5↑***** **RPL11 ↑***** **γ-H2A.X protein ↑**

	½ IC50		IC50	
Colon SW620	TGFβ1 — TGFβ2 — TGFβ3 — TGFβ3 protein — SMAD 1 — SMAD 2 — SMAD 2 protein — SMAD 3 — SMAD 4 — **SMAD 4 protein↓** **P53 ↑*** ATM — ATR — RPL5 — RPL11 — γ-H2A.X protein —	**TGFβ1 ↓***** TGFβ2 — TGFβ3 — TGFβ3 protein — **SMAD 1 ↓**** **SMAD 2 ↓***** SMAD 2 protein — **SMAD 3 ↓***** SMAD 4 — SMAD 4 protein — **P53 ↓***** **ATM ↓***** ATR — RPL5 — **RPL11 ↑***** **γ-H2A.X protein ↑**	**TGFβ1 ↑***** TGFβ2 — TGFβ3 — TGFβ3 protein — **SMAD 1 ↑***** **SMAD 2 ↑***** SMAD 2 protein — SMAD 3 — **SMAD 4 ↑**** SMAD 4 protein↓ **P53 ↑***** **ATM ↑***** **ATR ↑***** **RPL5 ↑***** **RPL11 ↑**** γ-H2A.X protein —	**TGFβ1 ↓***** TGFβ2 — TGFβ3 — TGFβ3 protein — **SMAD 1 ↓***** **SMAD 2 ↓***** SMAD 2 protein — **SMAD 3 ↓***** **SMAD 4 ↓***** SMAD 4 protein — **P53 ↓***** **ATM ↓***** **ATR ↓***** **RPL5 ↓***** **RPL11 ↓***** **γ-H2A.X protein ↑**

Discussion

PFOA and GenX cytotoxicity

GenX, initially developed as a safer alternative to PFOA (Zane and Schultz, 2020), exhibited higher IC_{50} values across all tested cell lines, indicating lower cytotoxicity. This observation is consistent with prior studies showing greater cytotoxicity for PFOA in immune cells such as THP-1 monocytes and Jurkat T-cells (McCall et al., 2024). Notably, contrasting results have been reported in thyroid models, where GenX demonstrated greater toxicity than PFOA (Zhang et al., 2021), pointing to tissue- and lineage-specific variability in PFAS response. While few

comparative studies have examined skin, kidney, and colon cell lines, the liver has traditionally served as a model for PFAS hepatotoxicity. Rat studies confirm PFOA's higher potency at matched external doses, yet suggest that internal target-organ dosimetry can equalize the effects of PFOA and GenX (Gomis et al., 2018). Therefore, our current findings should be contextualized as part of a broader toxicological framework that integrates both cytotoxicity and molecular response.

DNA Damage and p53 Pathway Activation

A key aim of our study was to examine whether the observed cytotoxicity was underpinned by genotoxic stress and DNA damage. In A375 skin cells, γ-H2A.X foci were present across all exposure levels, yet no dose-dependent pattern emerged. This may suggest a threshold response or alternatively reflect limitations of detection sensitivity at lower concentrations. Prior work by Peropadre et al. (2018) showed significant γ-H2A.X activation at 50 μM PFOA in skin keratinocytes after 24 hours of exposure and an extended recovery period, which may explain differences in observed patterns. Notably, Bouquet et al. (2006) emphasized that γ-H2A.X foci formation is an early event and may occur without a concurrent increase in protein expression detectable by immunoblotting, as used here.

In contrast to the skin, DNA damage markers were more dynamically regulated in metabolically active cells. In HepG2 and SN12C cells, γ-H2A.X expression increased in a concentration-dependent manner with both chemicals, consistent with genotoxic stress. Interestingly, in SW620 colon cells, GenX induced a pronounced γ-H2A.X response, while PFOA did not—suggesting that GenX may elicit DNA strand breakage more effectively in colonic epithelial cells. This pattern was echoed in the expression of upstream DNA damage regulators. In liver cells, both

PFOA and GenX upregulated ATM, ATR, and p53—central components of the DNA damage sensing and repair machinery. However, tissue-specific divergence emerged: in SN12C kidney cells, PFOA suppressed ATM/ATR and p53 expression, while GenX activated them. In the colon, the inverse pattern was observed, with PFOA inducing ATM/ATR/p53 upregulation and GenX causing downregulation. These discordant findings suggest chemical-specific differences in how DNA damage is detected and processed across tissues and warrant further studies exploring post-translational modifications of p53 (Hafner et al., 2019), including phosphorylation and acetylation, to better clarify its activation status.

Ribosomal Stress as a p53 Modulator

Given the interplay between ribosomal dysfunction and p53 activation, we also evaluated expression of ribosomal stress sensors RPL5 and RPL11. In A375 skin cells, both genes were significantly upregulated only under IC_{50} PFOA treatment, suggesting a stress threshold that triggers the nucleolar surveillance pathway. In contrast, HepG2 liver cells exhibited a clear and consistent increase in RPL5 and RPL11 across both treatments, corresponding with p53 upregulation and reinforcing the role of ribosomal stress in hepatic PFAS response (Li et al., 2022).

The kidney and colon cell lines again showed inverse responses to the two compounds. In SN12C cells, PFOA suppressed RPL5/RPL11 expression, while GenX upregulated both. In SW620 cells, PFOA elevated ribosomal stress markers, while GenX reduced them. These observations suggest that while GenX may more strongly disrupt ribosome homeostasis in the kidney, PFOA exerted greater ribosomal stress in the colon, possibly through differential impacts on nucleolar integrity or translation control.

TGF-β/SMAD Signaling and Inflammation

This study provides the first comparative analysis of TGF-β/SMAD pathway modulation by the perfluoroalkyl substances PFOA and GenX across hepatic, renal, and colonic cell lines. TGF-β signaling is a pivotal regulator of inflammation, fibrosis, and epithelial-to-mesenchymal transition (EMT), and its dysregulation has been implicated in both endocrine disruption and immune dysfunction (Bariani et al., 2023; Kehrl et al., 1986; Jobling et al., 2004). In HepG2 hepatocytes, both compounds induced robust transcriptional upregulation of SMAD2 and SMAD4; however, corresponding protein levels remained unchanged, suggesting that PFAS exposure may perturb translational efficiency or promote post-translational degradation, potentially via proteasomal or miRNA-mediated mechanisms.

Notably, distinct responses were observed in renal and colonic models. In SN12C kidney cells, PFOA suppressed TGF-β/SMAD gene expression, while GenX led to significant induction, suggesting compound-specific effects on renal inflammation or repair pathways. Conversely, in SW620 colonic cells, PFOA enhanced SMAD expression, whereas GenX inhibited it—indicating opposing regulatory dynamics that may reflect distinct cellular stress adaptations. These variations underscore the tissue-specific complexity of PFAS-induced signaling responses.

Canonical TGF-β signaling is initiated by ligand binding (TGF-β1, TGF-β2, or TGF-β3), leading to phosphorylation of receptor-regulated SMADs (R-SMADs, including SMAD2, SMAD3, and in some contexts, SMAD1), which then associate with the common-mediator SMAD4 and translocate to the nucleus to regulate target gene expression. In our study, transcriptional induction of SMAD2, SMAD3,

SMAD4, and in some cases SMAD1, coincided with marked upregulation of TGF-β1 and increased expression of DNA damage response markers such as γ-H2A.X, p53, ATM, and ATR. This co-activation suggests that SMAD signaling may be engaged in response to PFAS-induced genotoxic stress, coordinating cell cycle arrest with pro-apoptotic or DNA repair programs.

Intriguingly, despite the elevated transcript levels, SMAD2 and SMAD4 protein expression declined at higher toxin concentrations, consistent with possible post-transcriptional repression or proteolytic turnover under sustained stress. These findings align with the established profibrotic and oncogenic roles of TGF-β/SMAD signaling in chronic hepatic injury and support growing concerns regarding the hepatotoxic potential of both legacy and emerging PFAS compounds.

Conclusion

Taken together, our results demonstrate that while GenX exhibits lower overall cytotoxicity than PFOA, its impacts on DNA integrity, ribosomal stress, and inflammatory signaling are tissue- and pathway-specific. These findings challenge the assumption of universal safety among PFAS alternatives and underscore the need for molecular-level screening of replacement compounds. In terms of broader implications, persistent environmental exposure—particularly via drinking water and agricultural contamination—has been associated with PFAS blood levels exceeding Tolerable Daily Intakes (TDIs) (Gebbink and van Leeuwen, 2020). The differential accumulation patterns of these compounds also matter: GenX, due to its higher polarity and ether substitution, exhibits greater solubility and accumulation in water-rich matrices like plants, while PFOA preferentially partitions into lipophilic tissues and soils (Chen et al., 2019; Liu et al., 2021). Future studies should assess the

interplay of DNA damage, ribosomal integrity, and inflammation using systems-level approaches that integrate transcriptomic, proteomic, and phospho-proteomic data. Post-translational modifications of p53 and SMADs may provide crucial insight into the nuanced toxicodynamics of PFAS and support the development of targeted interventions and policy responses.

Appendix 1: List of materials

Cell lines	**Brand**	**Catalog Number**
A375	Pricella	CL-0014
HepG2	Pricella	CL-0103
SN12C	Pricella	CL-0744
SW620	Pricella	CL-0225B

Materials	**Brand**	**Catalog Number**
T25 Flasks	Corning, NY, USA	430168
T75 Flasks	Corning, NY, USA	3290
Incubator	Esco Micro Pte. Ltd, Singapore	CLM-240B-8-TC
Varioskan™ LUX plate reader	Thermo Fisher Scientific, MA, USA	
6-well plates	NEST, Wuxi, China	703003-ZX

Gel Electrophoresis System	Tanon, Shanghai, China	
Wet Transfer System	Tanon, Shanghai, China	
Chemiluminescence Imaging System	Bio-Rad Laboratories, CA, USA	
HiScript II 1st Strand cDNA Synthesis Kit	Vazyme, Nanjing, China	R212-01
Nanodrop	Thermo Fisher Scientific, MA, USA	840-317400
PCR thermal cycler	Bio-Rad Laboratories, CA, USA	
96-well PCR plates	NEST, Wuxi, China	
ChamQ Universal SYBR qPCR Master Mix	Vazyme, Nanjing, China	
GraphPad Prism	GraphPad Software, San Diego, CA	Version 9.5.1 for Windows

Chemicals	**Brand**	**Catalog Number**
Perfluorooctanoic acid	Aladdin	P106681
Perfluoro(2-methyl-3-oxahexanoic) acid	Aladdin	P302398
RIPA Lysis Buffer (Strong)	Beyotine	P0013B
Dulbecco's modified eagle medium (DMEM)	Gibco	C11995500BT
Fetal bovine serum (FBS)	Gibco	A5669701
Penicillin-Streptomycin (P/S)	Gibco	15070063
Trypsin-EDTA (0.25%) with phenol red	Gibco	25200056
Dimethyl sulfoxide (DMSO)	Solarbio	D8371
1M Tris pH 6.8	Quayad	QYR011
1M Tris pH 8.8	Quayad	QYR032
Sodium Dodecyl Sulfate (SDS)	BioFroxx	3250
Bovine Serum Albumin (BSA)	BioFroxx	4240
Tris-base	BioFroxx	1115
Glycine	BioFroxx	1275
Ammonium Persulfate (APS)	MACKlIN	A6295
N,N,N',N'-Tetramethylethylenediamine	MACKlIN	T6023
Tween 20	VETEC	V900548

Methanol	Adamas	75851G
Chloroform	Adamas	75915R
DEPC water	Adamas life	G8010
RNase-free ddH2O	Adamas life	G8051
PageRuler™ Prestained protein MW standard, 10 to 180 kDa	Thermo Fisher Scientific	26616
ECL WB substrate	Tanon	180-501
Trizol	Sigma-Aldrich Corporation	T9424
Phosphate Buffered Saline (PBS 1X)	Meilunbio	MA0015-1
HiScript II 1st Strand cDNA Synthesis Kit	Vazyme	R211-02
ChamQ Universal SYBR qPCR Master Mix	Vazyme	Q711-02
Enhanced Cell Counting Kit-8	Beyotime	C0042
30% Acr-Bis (29:1)	Beyotime	ST003
GAPDH Mouse mAb	Cell Signaling Technology	97166
Phospho-Histone H2A.X Rabbit mAb	Cell Signaling Technology	9718
Smad2 Rabbit Monoclonal Antibody	Beyotime	AF1300
SMAD4 Rabbit mAb	Abcam	ab40759
TGFβ3 Rabbit mAb	Abcam	ab308300

Appendix 2: Gel and Buffer Recipes

Separation Gel

Gradients	**Volume(mL)**			
10% gel	10.0	20.0	30.0	40.0
ddH_2O	2.7	5.3	8.0	10.6
30%Acr-Bis(29:1)	3.3	6.7	10.0	12.4
1 M Tris, pH8.8	3.8	7.6	11.4	15.2
10%SDS	0.1	0.2	0.3	0.4
10%APS	0.1	0.2	0.3	0.4
TEMED	0.004	0.008	0.012	0.016

Gradients	**Volume(mL)**			
15% gel	10.0	20.0	30.0	40.0
ddH_2O	1.0	2.0	3.0	4.0
30%Acr-Bis(29:1)	5.0	10.0	10.0	12.4
1 M Tris, pH8.8	3.8	7.6	11.4	15.2
10%SDS	0.1	0.2	0.3	0.4
10%APS	0.1	0.2	0.3	0.4
TEMED	0.004	0.008	0.012	0.016

Stacking Gel

Gradients	**Volume(mL)**			
15% gel	4.0	6.0	8.0	10.0
ddH_2O	2.7	4.1	5.5	6.8
30%Acr-Bis(29:1)	0.67	1.00	1.30	1.70
1 M Tris, pH8.8	0.50	0.75	1.00	1.25
10%SDS	0.04	0.06	0.08	0.10
10%APS	0.04	0.06	0.08	0.10
TEMED	0.004	0.006	0.008	0.010

Tris-Glycine running buffer

Tris base	3.024 g
Glycine	14.4 g
SDS	1 g
ddH_2O	1000mL

10x Transferring buffer

Tris base	30.2 g
Glycine	144 g
ddH_2O	1L

1x Transferring buffer

10x Transferring buffer	100 mL
Methanol	200 mL
ddH_2O	700 mL

10xTBS (Tris-buffered saline)

NaCl	160 g
Tris base	48 g
ddH_2O	2000mL

TBST (Tris-buffered saline with Tween 20)

10xTBS	100mL
Tween 20	1mL
ddH_2O	900mL

Appendix 3: Antibody Dilutions

Antibody	Dilution
GAPDH (primary)	1:1000
Smad2 (primary)	1:2000
Smad4 (primary)	1:5000
H2A.X (primary)	1:1000

TGFβ3 (primary)	1:1000
Goat anti-rabbit (secondary)	1:5000
Goat anti-mouse (secondary)	1:5000

Appendix 4: Q-PCR Primers

Gene	Primer sequence	Product size
ATM	F: GAGCAGAGTCTTGCCCTGAG	20
	R: TTTAGGCTGGGATTGTTCGCT	21
ATR	F: CCAGTGAAAGGGCATTCCAA	20
	R: GAACATGGGTCTTGGCCTTTT	21
$TGF\beta_1$	F: GGAAATTGAGGGCTTTCGCC	20
	R: CCGGTAGTGAACCCGTTGAT	20
$TGF\beta_2$	F: CGAGAGGAGCGACGAAGAGT	20
	R: ACAACTGGGCAGACAGTTTCG	21
$TGF\beta_3$	F: GGAAAACACCGAGTCGGAATAC	22
	R: GCGGAAAACCTTGGAGGTAAT	21
SMAD1	F: CCGATGGACACAAACATGATGGC	23
	R: AAGCAACCGCCTGAACATCTCC	22
SMAD2	F: GTCCATCTTGCCATTCACG	19
	R: CTCAAGCTCATCTAATCGTCCTG	23
SMAD3	F: AAGGACGAGGTCTGCGTGAATC	22
	R: CCAACACAGGAGGTAGAACTGGTG	24
SMAD4	F: TCCTGTGGCTTCCACAAGTCAG	22
	R: GCCCTGATGCTATCTGCAACAGTC	24
RPL5	F: CAACACACCCAAATACAGGATG	22
	R: CGGGCATAAGCAATCTGACAA	21
RPL11	F: GTCCACTGCACAGTTCGAGG	20
	R: AACTCATACTCCCGCACCTTT	21
p53	F: CAGCACATGACGGAGGTTGT	20
	R: TCATCCAAATACTCCACACGC	21
GAPDH	F: ACAACTTTGGTATCGTGGAAGG	22
	R: GCCATCACGCCACAGTTTC	19

All primers were synthesized by AZENTA Life Sciences (Suzhou, China).

References

1. Ahearn A. A Regrettable Substitute: The Story of GenX. Podcasts: The Researcher's Perspective. 2019; 2019(1). https://doi.org/10.1289/EHP5134
2. Abudayyak M, Öztaş E, Özhan G. Determination of perfluorooctanoic acid toxicity in a human hepatocarcinoma cell line. J Health Pollut. 2021;11(31):210909. https://doi.org/10.5696/2156-9614-11.31.210909

3. Bariani, M. V., Cui, Y. H., Ali, M., Bai, T., Grimm, S. L., Coarfa, C., ... & Al-Hendy, A. (2023). TGFβ signaling links early life endocrine-disrupting chemicals exposure to suppression of nucleotide excision repair in rat myometrial stem cells. *Cellular and Molecular Life Sciences*, *80*(10), 288.
4. Bouquet F, Muller C, Salles B. The Loss of γH2AX Signal is a Marker of DNA Double Strand Breaks Repair Only at Low Levels of DNA Damage. Cell Cycle. 2006;5(10):1116–22.https://doi.org/10.4161/cc.5.10.2799.
5. Buck RC, Franklin J, Berger U, et al. Perfluoroalkyl and polyfluoroalkyl substances in the environment: Terminology, classification, and origins. Integr Environ Assess Manag. 2011;7(4):513-541. https://doi.org/10.1002/ieam.258
6. Chen, C., Yang, S., Liu, Y., Jamieson, P., Shan, L., & Chu, K., 2019. Accumulation and phytotoxicity of perfluorooctanoic acid and 2,3,3,3-tetrafluoro-2-(heptafluoropropoxy)propanoate in Arabidopsis thaliana and Nicotiana benthamiana.. Environmental pollution, 259, pp. 113817 . https://doi.org/10.1016/j.envpol.2019.113817.
7. Conley JM, Lambright CS, Evans N, et al. Adverse maternal, fetal, and postnatal effects of hexafluoropropylene oxide dimer acid (GenX) from oral gestational exposure in Sprague-Dawley rats. Environ Health Perspect. 2019;127(3):037008. https://doi.org/10.1289/EHP4372
8. De Silva AO, Armitage JM, Bruton TA, et al. PFAS exposure pathways for humans and wildlife: A synthesis of current knowledge and key gaps in understanding. Environ Toxicol Chem. 2021;40(3):631-657. https://doi.org/10.1002/etc.4935
9. Ehsan, M., Riza, M., Pervez, M., Khyum, M., Liang, Y., & Naddeo, V., 2023. Environmental and health impacts of PFAS: Sources, distribution and sustainable management in North Carolina (USA).. The Science of the total environment, pp. 163123 https://doi.org/10.1016/j.scitotenv.2023.163123.
10. Gandhi V, O'Brien MH, Yadav S. High-quality and high-yield RNA extraction method from whole human saliva. Biomark Insights. 2020;15:1177271920929705. https://doi.org/10.1177/1177271920929705
11. Gebbink, W.A. and van Leeuwen, S.P.J. (2020). Environmental contamination and human exposure to PFASs near a fluorochemical production plant: Review of historic and current PFOA and GenX contamination in the Netherlands. Environment International, 137, p.105583. doi:https://doi.org/10.1016/j.envint.2020.105583.
12. Gomis MI, Vestergren R, Borg D, Cousins IT. Comparing the toxic potency in vivo of long-chain perfluoroalkyl acids and fluorinated alternatives. Environ Int. 2018;113:1-9. https://doi.org/10.1016/j.envint.2018.01.011
13. Hafner A, Bulyk ML, Jambhekar A, Lahav G. The multiple mechanisms that regulate p53 activity and cell fate. Nature Reviews Molecular Cell Biology. 2019;20(4):199–210. https://doi.org/10.1038/s41580-019-0110-x.
14. Hu K, Fu M, Wang J, et al. HSV-2 infection of human genital epithelial cells upregulates TLR9 expression through the SP1/JNK signaling pathway. Front Immunol. 2020;11:356. https://doi.org/10.3389/fimmu.2020.00356
15. Jin, Y., Liu, W., Sato, I., Nakayama, S., Sasaki, K., Saito, N., & Tsuda, S.. PFOS and PFOA in environmental and tap water in China. Chemosphere. 2009;77(5):605-611 . https://doi.org/10.1016/j.chemosphere.2009.08.058.
16. Jobling, AI, Nguyen, M, Gentle, A, & McBrien, NA. Isoform-specific changes in scleral transforming growth factor-β expression and the regulation of collagen synthesis during myopia progression. Journal of Biological Chemistry. 2004;279(18):18121–18126. https://doi.org/10.1074/jbc.M400381200
17. Kehrl, JH, Roberts, AB, Wakefield, LM, Jakowlew, S, Sporn, MB, & Fauci, AS. Transforming growth factor beta is an important immunomodulatory protein for human B lymphocytes. Journal of Immunology, 1986;137(12):3855–3860. https://doi.org/10.4049/jimmunol.137.12.3855
18. Kwiatkowski CF, Andrews DQ, Birnbaum LS, et al. Scientific basis for managing PFAS as a chemical class. Environ Sci Technol Lett. 2020;7(8):532-543.

https://doi.org/10.1021/acs.estlett.0c00255
19. Li H, Zhang H, Huang G, Bing Z, Xu D, Liu J, Luo H, An X. Loss of RPS27a expression regulates the cell cycle, apoptosis, and proliferation via the RPL11-MDM2-p53 pathway in lung adenocarcinoma cells. J Exp Clin Cancer Res. 2022;41(1):33. https://doi.org/10.1186/s13046-021-02230-z
20. Lin CY, Lin LY, Wen TW, Lien GW, Chien KL, Hsu SHJ, Liao CC, Sung FC, Chen PC, Su TC. Association between levels of serum perfluorooctane sulfate and carotid artery intima-media thickness in adolescents and young adults. Int J Cardiol. 2013;168(4):3309-3316. https://doi.org/10.1016/j.ijcard.2013.04.042
21. Liu, B., Zhang, R., Zhang, H., Yu, Y., Yao, D., & Yin, S. (2020). Levels of Perfluoroalkyl Acids (PFAAs) in Human Serum, Hair and Nails in Guangdong Province, China: Implications for Exploring the Ideal Bio-Indicator. *Archives of Environmental Contamination and Toxicology*, *79*(2), 184–194. https://doi.org/10.1007/s00244-020-00743-w
22. Liu, Z., Xu, C., Johnson, A., Sun, X., Ding, X., Ding, D., Liu, S., & Liang, X., 2021. Source apportionment and crop bioaccumulation of perfluoroalkyl acids and novel alternatives in an industrial-intensive region with fluorochemical production, China: Health implications for human exposure.. Journal of hazardous materials, 423 Pt A, pp. 127019 . https://doi.org/10.1016/j.jhazmat.2021.127019.
23. Massagué J. TGFβ signalling in context. 2012;13:616–630. https://doi.org/10.1038/nrm3434.
24. McCall JR, Sausman KT, Brown AP, Mead RN. In vitro cytotoxicity of six per- and polyfluoroalkyl substances (PFAS) in human immune cell lines. Toxicology in Vitro. 2024 Oct 1;100:105910–0. https://doi.org/10.1016/j.envint.2021.106745.
25. Omotola, E, Olatunji, O., & Moodley, B., 2024. Trace detection of perfluorooctanoic acid and perfluorooctane sulfonate in surface sediments using a liquid chromatograph coupled to an electrospray ionization single quadrupole mass spectrometer (LC-ESI–Q-MS). Microchemical Journal. https://doi.org/10.1016/j.microc.2024.109928.
26. Peropadre A, Fernández Freire P, Hazen MJ. A moderate exposure to perfluorooctanoic acid causes persistent DNA damage and senescence in human epidermal HaCaT keratinocytes. Food and Chemical Toxicology. 2018 Sep 12;121:351–9. https://doi.org/10.1016/j.fct.2018.09.020.
27. Poothong, S., Papadopoulou, E., Padilla-Sánchez, J. A., Thomsen, C., & Haug, L. S. (2020). Multiple pathways of human exposure to poly- and perfluoroalkyl substances (PFASs): From external exposure to human blood. *Environment International*, *134*, 105244. https://doi.org/10.1016/j.envint.2019.105244
28. Shen, Y. et al. TGF-β1 downregulates ATM and impairs the DNA damage response in ovarian cancer cells. PLoS One 9, e107296 (2014). https://doi.org/10.1371/journal.pone.0107296
29. Sunderland EM, Hu XC, Dassuncao C, Tokranov AK, Wagner CC, Allen JG. A review of the pathways of human exposure to poly- and perfluoroalkyl substances (PFASs) and present understanding of health effects. J Expo Sci Environ Epidemiol. 2019;29(2):131-147. https://doi.org/10.1038/s41370-018-0094-1
30. Ubel FA, Sorenson SD, Roach DE. Health status of plant workers exposed to fluorochemicals—A preliminary report. Am Ind Hyg Assoc J. 1980;41(8):584-589. https://doi.org/10.1080/15298668091425310
31. Wee SY, Aris AZ. Revisiting the "forever chemicals", PFOA and PFOS exposure in drinking water. npj Clean Water. 2023; https://doi.org/10.1038/s41545-023-00274-6
32. Xiao, F, Simcik, M, Halbach, T, & Gulliver, J. Perfluorooctane sulfonate (PFOS) and perfluorooctanoate (PFOA) in soils and groundwater of a U.S. metropolitan area: migration and implications for human exposure. Water research. 2015; 72:64-74 . https://doi.org/10.1016/j.watres.2014.09.052.
33. Yoo HJ, et al. Hexafluoropropylene oxide dimer acid (GenX) exposure induces apoptosis in HepG2 cells. Heliyon. 2021;7(11).

https://doi.org/10.1016/j.heliyon.2021.e08272
34. Zane L, Schultz T. Cytotoxicity of environmental toxins PFOA and Gen X. Ocean Sciences Meeting 2020.
35. Zhang S, Chen K, Li W, Chai Y, Zhu J, Chu B, Li N, Yan J, Zhang S, Yang Y. Varied thyroid disrupting effects of perfluorooctanoic acid (PFOA) and its novel alternatives hexafluoropropylene-oxide-dimer-acid (GenX) and ammonium 4,8-dioxa-3H-perfluorononanoate (ADONA) in vitro. Environ Int. 2021;156:106745. https://doi.org/10.1016/j.envint.2021.106745

Statements and Declarations

Funding
This work was supported by Duke Kunshan University Discretionary funds, Undergraduate studies research funds, Signature Work Research fund, Global Health Graduate School funds, and Seed Wang foundations.

Competing Interests
The authors have no relevant financial or non-financial interests to disclose.

Author Contributions
Hongran Ding and Anastasia Tsigkou contributed to the study conception and design. Data collection and analysis were performed by Hongran Ding and Bo Chen.
Hongran Ding drafted the manuscript. Maya Slack, Holly McClure, Wen Gu, Carly Nabinger, Renata Koviazina, and Helene Gu revised the manuscript. The graphical abstract was designed by Holly McClure. All authors read and approved the final manuscript. Jason Somarelli, Thomas Schultz, Anastasia Tsigkou, and Ferdinand Kappes supervised this project.

Acknowledgements
The authors would like to acknowledge Marius Wamsiedel and Chenkai Wu for their supervision of the Global Health Program.